

# Gating currents of the cloned delayed-rectifier K<sup>+</sup> channel DRK1

(*Xenopus* oocytes)

MAURIZIO TAGLIALATELA AND ENRICO STEFANI\*

Department of Molecular Physiology and Biophysics, Baylor College of Medicine, One Baylor Plaza, Houston, TX 77030

Communicated by Clay M. Armstrong, December 24, 1992

**ABSTRACT** Gating currents of the cloned delayed-rectifier K<sup>+</sup> channel DRK1 expressed in *Xenopus* oocytes were measured with the open-oocyte Vaseline-gap voltage-clamp technique. DRK1 gating charge had the following salient properties: (i) gating-charge amplitude correlated positively with size of the expressed ionic K<sup>+</sup> currents; (ii) the time integral of ON and OFF gating currents was similar, indicating charge conservation and lack of charge immobilization; (iii) the gating-charge activation curve was shallower and had a half-activation potential 15 mV more negative than the activation curve for K<sup>+</sup> conductance; (iv) effective valence for the gating current was about two electronic charges per gating subunit; (v) for large depolarizations (to >0 mV) prominent rising phases were observed during the ON and OFF gating charge, which appeared as shoulders in unsubtracted traces; (vi) for small depolarizing pulses (to <0 mV) ionic-current activation and deactivation had time constants similar to ON and OFF gating-current decay, respectively; (vii) negative prepulses made more prominent the ON rising phase and delayed ionic and gating currents. The results are consistent with a model for K<sup>+</sup> channel activation that has an early slow and/or weakly voltage-dependent transition between early closed states followed by more voltage-dependent transitions between later closed states and a final voltage-independent closed–open transition.

In voltage-dependent ion channels, gating currents are generated by the displacement of voltage-sensing elements as a consequence of changes in the membrane electric field (1–5). Recent work has described isolated gating properties of Shaker B K<sup>+</sup> channels (6). In the present study, we further characterize K<sup>+</sup> gating-current kinetics in unsubtracted records from another cloned voltage-dependent K<sup>+</sup> channel (DRK1) with delayed-rectifier properties (7). To improve the recording of gating currents we increased the performance of the open-oocyte Vaseline-gap voltage-clamp technique (8) to allow control of the ionic composition at both sides of the oocyte membrane.

## MATERIALS AND METHODS

**DRK1 Channel Expression in Oocytes.** The cloning of DRK1 cDNA from a directional rat brain cDNA library, as well as DRK1 cRNA preparation and oocytes injection and handling, has been described (7).

**Solutions.** The solutions used in the present experiments were the following: 88 mM NaCl/1 mM KCl/2.4 mM NaHCO<sub>3</sub>/15 mM sodium Hepes/0.3 mM Ca(NO<sub>3</sub>)<sub>2</sub>/0.4 mM CaCl<sub>2</sub>/0.8 mM MgSO<sub>4</sub>, pH 7.6 (Barth); 120 mM KCH<sub>3</sub>SO<sub>3</sub>/10 mM sodium Hepes, pH 7.3 (K-Mes); 107 mM TEA-CH<sub>3</sub>SO<sub>3</sub>/5 mM Mg(CH<sub>3</sub>SO<sub>3</sub>)<sub>2</sub>/5 mM sodium Hepes, pH 7.3 (Mg-TEA-Mes); 107 mM TEA-CH<sub>3</sub>SO<sub>3</sub>/5 mM Ca(CH<sub>3</sub>SO<sub>3</sub>)<sub>2</sub>/5 mM sodium Hepes, pH 7.3 (Ca-TEA-Mes), where TEA is tetraethylammonium, Mes is 2-(*N*-morpholi-

no)ethanesulfonic acid, and Hepes is 4-(2-hydroxyethyl)-1-piperazineethanesulfonic acid.

**Recording of Macroscopic and Gating Currents with the Open-Oocyte Vaseline-Gap Voltage-Clamp.** The experimental chamber and the electronic apparatus used to record ionic and gating currents have been described (8). In these present experiments we further improved the system dynamic by actively clamping the guard-shield compartment. Recorded pulse potentials closely followed the command pulse that was rounded with a time constant of 30 μs. Signals were filtered at one-fourth the sampling frequency (10–50 kHz). Linear capacity and resistive components were digitally subtracted with negative pulses one-fourth of the amplitude of the test pulse and from –120 mV. Gating currents (averages of 4–10 sweeps) were normalized per input capacity.

## RESULTS

**Ionic and Gating Currents of DRK1 Channels.** Fig. 1A shows capacitive currents in response to a 20-mV pulse. At 50-kHz recording bandwidth the current settles in ≈300 μs with a time constant (40 μs) similar to that of the command pulse. With the present improvements in the clamp speed the charging process of the membrane follows a fast single exponential curve, and the slower component previously described (8) was absent.

*Xenopus* oocytes injected with cRNA encoding DRK1 channels expressed voltage-dependent K<sup>+</sup>-selective currents with delayed-rectifier properties that activated ≈–30 mV (Fig. 1B). Fig. 1C shows subtracted current responses to the indicated test potentials after blockade of K<sup>+</sup> ionic currents by replacing internal K-Mes and external Barth solutions with Mg-TEA-Mes and Ca-TEA-Mes solutions, respectively. DRK1 K<sup>+</sup> current kinetics recorded during development of the TEA block remained practically unmodified (8, 9). This result agrees with the view that TEA acts as an open-channel blocker with very fast ON and OFF rates compared with channel mean open and closed times (10, 11). TEA-resistant currents had the properties of K<sup>+</sup> gating currents. They were detected at potentials more negative than the ionic K<sup>+</sup> currents and increased in amplitude with depolarization, reaching saturation at positive potentials. We never observed transient currents like those in Fig. 1C in uninjected oocytes. Furthermore, a positive correlation was found between the peak values of the expressed ionic current and of the transient current remaining after TEA block. This result indicates that the transient currents were related to the presence of functional DRK1 channels and that the transient ON and OFF currents correspond to the ON and OFF gating-charge movements of DRK1 channels. Gating currents were adequately recorded in oocytes with a limiting K<sup>+</sup> conductance (*g*K<sup>+</sup>) of ≈30 mS/cm<sup>2</sup>, assuming 1 μF = 1 cm<sup>2</sup>. The corresponding maximum gating-charge values were 5–10 nC/cm<sup>2</sup>. Similar

The publication costs of this article were defrayed in part by page charge payment. This article must therefore be hereby marked "advertisement" in accordance with 18 U.S.C. §1734 solely to indicate this fact.

Abbreviations: TEA, tetraethylammonium; *g*K<sup>+</sup>, K<sup>+</sup> conductance; QK<sup>+</sup><sub>v</sub>, gating-charge steady-state activation.

\*To whom reprint requests should be addressed.

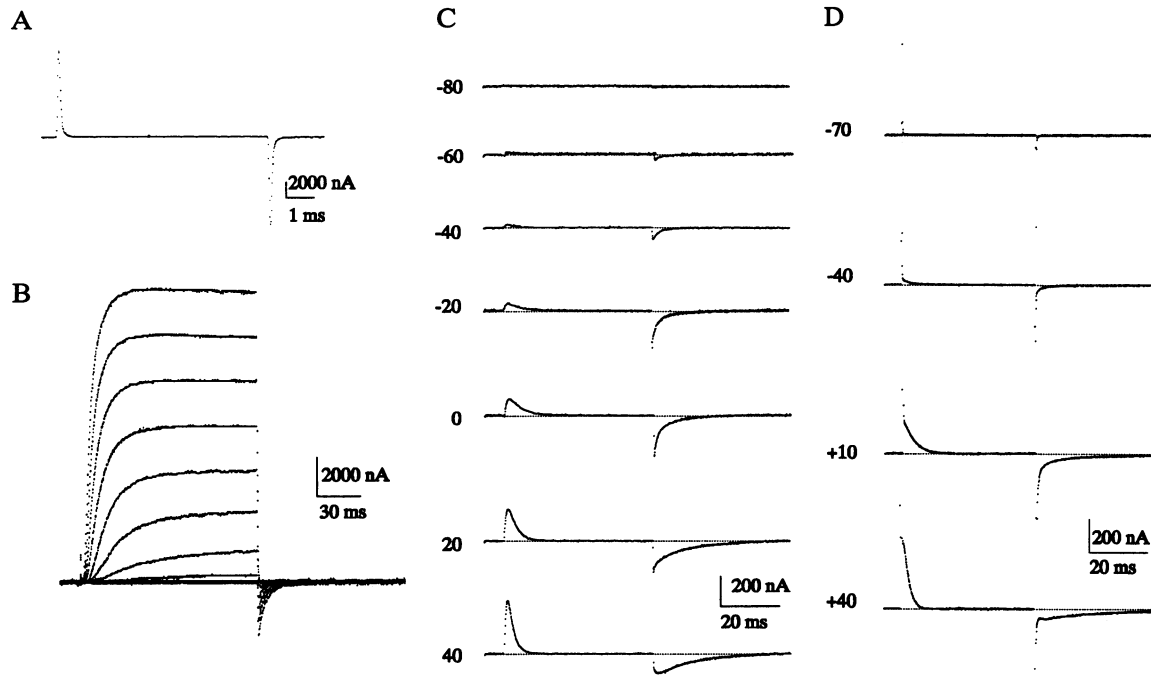


FIG. 1. DRK1 ionic and gating currents. (A) Capacity transients to 20-mV step. (B) Macroscopic currents. Holding potential was  $-80$  mV; pulses were from  $-60$  to  $+40$  mV in 10-mV steps. External and internal solutions were Barth solution with 8 mM KCl and with K-Mes, respectively. (C) Gating currents. Holding potential was  $-100$  mV. External and internal solutions were Ca-TEA-Mes and Mg-TEA-Mes, respectively. (D) Unsubtracted records of DRK1 capacity and gating currents; holding potential was  $-80$  mV, and solutions were as in C.

values were reported for  $K^+$  gating current and  $gK^+$  in the squid axon (12).

DRK1 gating currents at the beginning of the depolarizing pulse had a rising phase and a plateau that was followed by a slower exponential decay which became faster with depolarization. Upon repolarization to the holding potential, the OFF gating current had also a detectable rising phase with a plateau only for large depolarizations (to  $>+20$  mV) (Fig. 1C and 2B). ON and OFF gating currents were not modified by varying the polarity of the subtracting control pulses and the subtracting holding potential from  $-90$  mV to  $-120$  mV.

Fig. 1D shows unsubtracting records from another oocyte after the blockade of  $K^+$  currents. The capacity charging process is fast enough to allow separation of the linear membrane capacity from ON and OFF gating charge. In these records the linear capacity transients are a few points off-scale. Unsubtracted gating currents had properties similar to those described in subtracted records. The shoulders in the ON and the OFF responses at  $+40$  mV correspond to the rising phases. The possibility that the reported rising phase of gating currents can be explained by the time course of the capacity charging process seems unlikely because the decay time constant of the capacity transient is much faster than the gating-charge rising-phase time constant ( $20$ – $40$   $\mu$ s and  $200$ – $400$   $\mu$ s, respectively). Furthermore in Fig. 1C for pulses from  $-20$  to  $20$  mV, the rising phase could be clearly resolved only at the ON response, whereas at the OFF response the initial return was quasi-instantaneous.

**Absence of Charge Immobilization in DRK1 Gating Currents.** Fig. 2 shows ON and OFF gating-current responses to depolarizing pulses to  $0$  mV (Fig. 2A) and  $+60$  mV (Fig. 2B) of increased duration. Time integrals of the ON and OFF gating currents plotted against length of the pulse (Fig. 2C) were identical, reaching saturation for longer depolarizing pulses, indicating the absence of charge immobilization. Fig. 2D shows the relationship between the time integral of the ON vs. OFF gating currents in six different cells for 50- to 125-ms pulses to various potentials ( $-60$  to  $+15$  mV). The experi-

mental points follow the line that indicates the equality between ON and OFF charges.

For pulses to  $0$  mV, the OFF gate relaxes with similar kinetics for all pulse durations. On the other hand, when the voltage was stepped to  $+60$  mV, the OFF relaxation kinetics depends on the pulse duration: for short pulses no rising phase was detected, while, as the pulse length increased, a rising phase became more prominent, and the decay phase became slower. Despite these kinetic changes, the ON and OFF time integrals remained equal. A similar rising phase in the OFF gating response, which develops for large depolarizations (to  $>-30$  mV) and longer test pulses, has been described for Shaker B  $K^+$  channels (13). However in Shaker B  $K^+$  channels internal TEA greatly slowed down OFF-charge relaxation inducing charge immobilization, whereas in DRK1  $K^+$  channels, even in the presence of isotonic internal TEA, the OFF charge was not immobilized.

**Steady-State and Kinetic Properties of DRK1 Ionic and Gating Currents.** Fig. 3A shows normalized DRK1 steady-state activation curves for the  $gK^+$  ( $\bullet$ ) and ON ( $\blacktriangle$ ) and OFF ( $\blacksquare$ ) gating charge.  $gK^+$  was determined from the steady-state current-voltage relationship (14) after correction for the instantaneous current-voltage rectification, as predicted by the Goldman-Hodgkin-Katz relationship (15). The experimental points were fitted to the Boltzmann equation,  $gK^+_{\nu} = 1/(1 + \exp(ze(V - V_{1/2})/kT))$ , where  $V$  is the pulse potential,  $V_{1/2}$  is the half-activation potential,  $z$  is the effective valence, and  $e$ ,  $k$ , and  $T$  are usual thermodynamic constants. The fitted values for  $V_{1/2}$  and  $z$  were  $-12.7 \pm 2.1$  mV and  $2.63 \pm 0.1$ , respectively ( $n = 7$ , mean  $\pm$  SEM). This effective valence corresponds to a lower estimate of electronic charges per channel moved before channel opening. Gating-charge steady-state activation ( $QK^+_{\nu}$ ) curves were obtained by integrating the first 50 ms of ON and OFF responses at different potentials. The experimental points were fitted to the same Boltzmann equation, replacing  $gK^+_{\nu}$  by  $QK^+_{\nu}$ . The fitted values for  $V_{1/2}$  and  $z$  were  $-24.0 \pm 4.0$  mV and  $2.17 \pm 0.3$  ( $n = 5$ ) for the ON and  $-28.0 \pm 1.0$  mV and  $2.05 \pm 0.2$  ( $n = 3$ ) for the OFF, respectively. The fact that  $V_{1/2}$  is  $\approx 15$  mV more

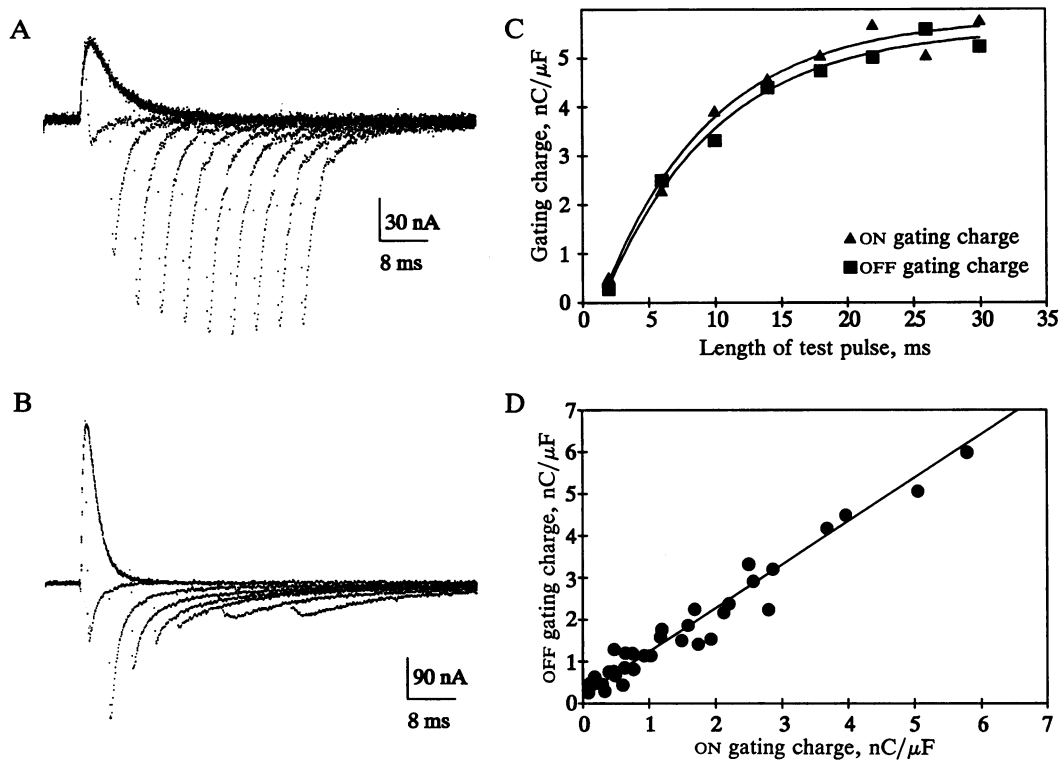


FIG. 2. Properties of DRK1 gating currents. (A and B) ON and OFF gating currents in response to 0-mV (A) and +60-mV (B) pulses of different durations. Holding potential was  $-80$  mV. External and internal solutions were Ca-TEA-Mes and Mg-TEA-Mes, respectively. (C) Relationship between time integrals of ON and OFF gating responses and pulse length. (D) Relationship between ON and OFF integrals for 50- to 125-ms pulses from  $-60$  to  $+15$  mV in six different oocytes. External and internal solutions were Ca-TEA-Mes and Mg-TEA-Mes, respectively.

negative in the  $QK^+_v$  curve than in the  $gK^+_v$  curve indicates that charge moves during transitions among the closed states before channel opening (4, 5). Fig. 3A reveals that the  $QK^+_v$  curves for ON and OFF are shallower than the  $gK^+_v$  curve. Furthermore the experimental points of the  $QK^+_v$  curve were more adequately described by the Boltzmann function than in the  $gK^+_v$  curve. This result becomes more evident at negative potentials ( $-50$  to  $-30$  mV), where the experimental values of the  $gK^+_v$  curve had a steeper voltage dependence than the fitted curve. Thus, we used smaller depolarizing steps (2 mV) to study ionic-current activation at those negative potentials where  $gK^+$  had steeper potential sensitivity (16). This foot region of the  $gK^+_v$  curve is well described by the exponential function  $gK^+_v/gK^+_{max} = A \exp(-zFV/RT)$ , where  $gK^+_{max}$  is the limiting  $gK^+$  and  $A$  is an amplitude factor (Fig. 3B, ●) (12). The fitted value of  $3.3 \pm 0.16$  ( $n = 10$ ) for  $z$  in the  $gK^+_v$  curve sets the lower limit for the total amount of elementary charges moved. A similar analysis for the  $QK^+_v$  curve [Fig. 3B, ▲ (ON) and ■ (OFF)] gives a smaller  $z$  of 2.1, which is very similar to the one obtained by fitting the Boltzmann function in the entire voltage range.

Fig. 3C shows DRK1 ON and OFF ionic and gating currents and superimposed fitted traces to single exponentials for a 0 mV pulse from  $-80$  mV holding potential. The time constants for activation and deactivation of the macroscopic current closely matched the corresponding values of the ON and OFF gating-charge responses. A similar correspondence was obtained from measurements performed over a wide range of potentials ( $-30$  to  $+50$  mV; Fig. 3D). For OFF gating-currents pulses to 0 mV were used because, as previously described, for larger depolarizations the kinetics of the gating-current relaxation depended on the pulse duration.

**Cole-Moore Phenomenon in DRK1 Ionic and Gating Currents.** Fig. 4A shows DRK1  $K^+$  currents to  $+40$  mV pulses preceded by 100-ms conditioning prepulses to  $-140$  and  $-60$

mV. Activation of the ionic current was delayed by the more negative prepulse (17). Fig. 4B and C shows ON gating currents to  $+40$  mV (B) and 0 mV (C) with same prepulse potentials. The  $-140$ -mV prepulse delayed and made more prominent the rising phase of the ON gating charge without recruiting additional charge. When the  $-60$ -mV prepulse was applied, the ON response appeared earlier, and the slow rising phase was preceded by a faster component that was probably limited in speed by the clamp frequency response. These results are in agreement with the  $QK^+_v$  (Fig. 3A), which shows undetectable charge movement at potentials  $> -60$  mV, and suggest the presence of initial less voltage-dependent states.

## DISCUSSION

Transient outward and inward currents recorded in DRK1-injected oocytes after ionic-current blockade with TEA can be regarded as DRK1 gating currents because they were never observed in uninjected oocytes and their amplitude had a positive correlation with the ionic-current level expressed. Furthermore, these currents had some general properties of gating currents. ON gating currents precede ionic-current activation, and the time integral of ON and OFF gating currents increased with voltage, saturating at positive potentials. In addition, the gating charge-activation curve was shallower and had a half-activation potential more negative than the activation curve for the  $gK^+$ . These findings suggest that charge movement between several closed states precedes channel opening.

The limiting values of the effective valence for  $gK^+$  give a lower estimate of the total amount of charge required to reach the open state (12, 16). On the other hand, for independent and identical gating subunits with two states, the effective valence of the  $QK^+_v$  curve corresponds to the amount of charge per gating element. Following these considerations,

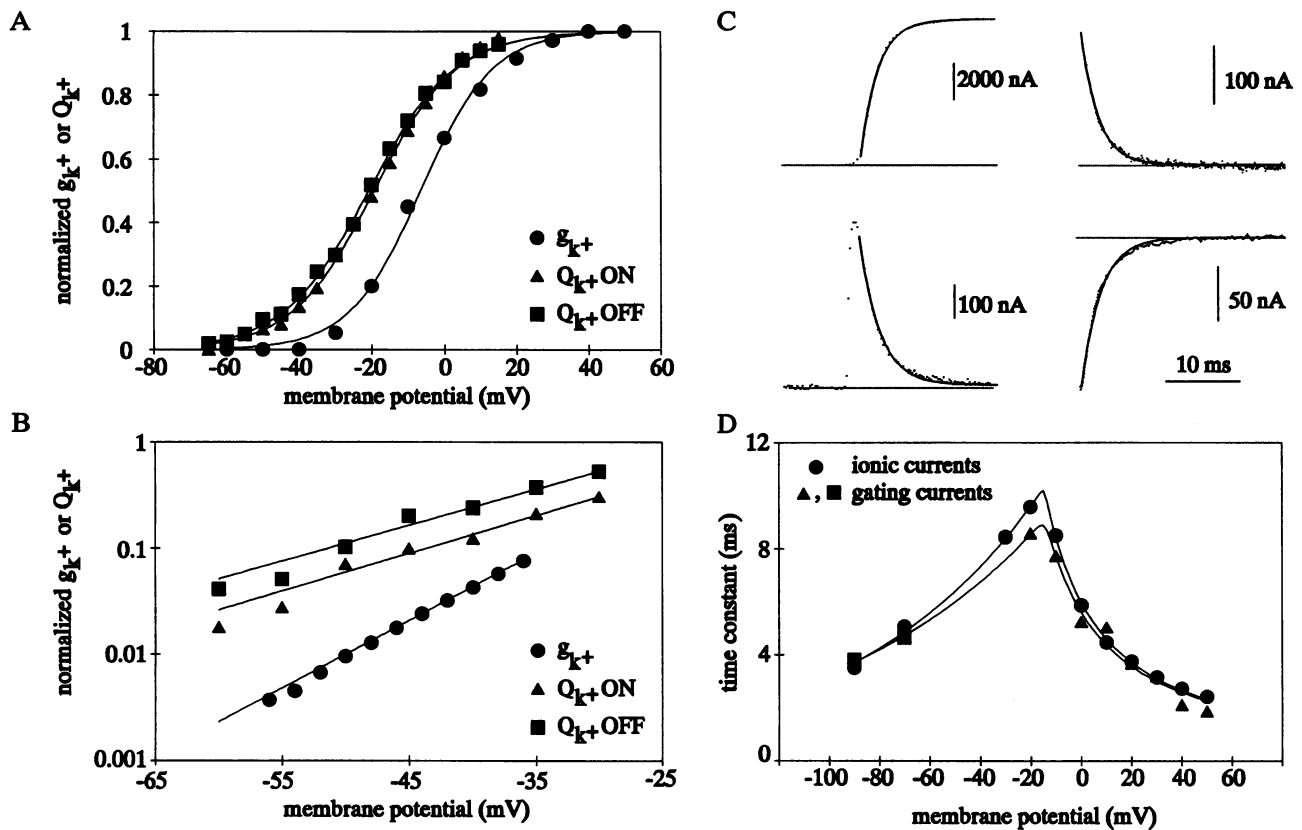


FIG. 3. Steady-state and kinetic properties of the ionic and gating currents of DRK1 channels. (A) Normalized  $g_{K^+}$  and gating-charge steady-state activation ( $Q_{K^+}$ ) relationships for DRK1 channels. Solid lines are best fits of the data to the Boltzmann distribution. (B) Semilogarithmic plot of normalized  $g_{K^+}$  and  $Q_{K^+}$  values vs. pulse potentials. Solid lines are the best fit to an exponential function describing the foot of the Boltzmann distribution (effective valences:  $g_{K^+} = 3.7$ ;  $Q_{K^+ ON}$  and  $OFF = 2.1$ ). (C) Superimposed single-exponential fits with ionic and gating currents from the same oocyte. Pulses to 40 mV [ionic current activation and ON gating current (Left)] or to 0 mV [ionic current deactivation and OFF gating current (Right)] from  $-80$  mV holding potential. (D) Relationship between ionic and gating-current time constants and membrane potential. Solid lines represent the best fit to the predicted time constant of a two-state model, assuming that ON and OFF rate constants vary exponentially with voltage. Ionic-current time constants ( $\bullet$ ) were obtained from deactivation ( $-90$  mV and  $-70$  mV) and activation ( $-30$  mV to  $+50$  mV) of  $K^+$  currents. Gating-current time constants were obtained from decay of the OFF ( $\blacksquare$ ,  $-90$  mV and  $-70$  mV) and of the ON ( $\blacktriangle$ ,  $-20$  mV to  $+50$  mV) responses. The solutions were as follows (external and internal, respectively): Barth solution and K-Mes for ionic currents and Ca-TEA-Mes and Mg-TEA-Mes for gating currents.

the ratio between the values of the effective valence of the  $g_{K^+}$  and  $Q_{K^+}$  curves (3.3 and 2.0, respectively) suggests in DRK1 a minimum estimate of approximately two (1.7) gating elements required to activate the  $g_{K^+}$  (16). A direct measurement of the number of electronic charges (12.4) per channels in Shaker B channels has been recently obtained from gating current and number of channel measurements with fluctuation analysis (18), which reasonably agrees with

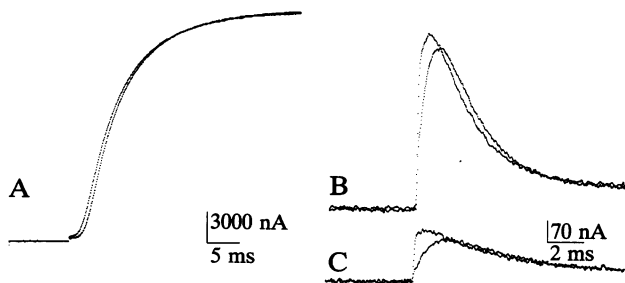


FIG. 4. Cole-Moore phenomenon in DRK1 ionic and gating currents. (A) DRK1 ionic currents in response to  $+60$ -mV pulses after 100-ms prepulses to  $-140$  mV or  $-60$  mV. Holding potential was  $-80$  mV. External and internal solutions were Barth solution and K-Mes, respectively. (B and C) ON gating currents recorded from the same cell in response to 0-mV (C) and  $+40$ -mV (B) pulses with the same prepulses as in A. External and internal solutions were Ca-TEA-Mes and Mg-TEA-Mes, respectively.

our predicted value (eight electronic charges), on the assumption that DRK1 channels assemble as tetramers of identical subunits (19) with one gating element per subunit. The fact that the number of calculated gating elements necessary for channel opening is less than the number of subunits can be explained either by an underestimated measurement of the limiting slope conductance and/or by cooperativity among the gating subunits. Nonindependent subunit gating agrees with the presence of a rising phase in the gating charge (6) and has been recently proposed for heterotetrameric RCK channels (20).

In the squid axon the OFF/ON ratio of the  $Na^+$  gating-current time integral is reduced by 50–70% when the depolarizing pulse length is increased from 0.3–1 ms to 10–20 ms (3, 21, 22). This phenomenon of charge immobilization has also been observed in gating currents measured from oocytes expressing  $K^+$  channels from *Drosophila* and rat brain (6, 23). In contrast, DRK1 OFF gating charge, as in the squid axon delayed-rectifier (4, 12), does not show any charge immobilization, even when 125-ms pulses to  $+15$  mV were used. Furthermore, internal TEA increased the degree of charge immobilization in Shaker B channels (6), whereas, in our recording conditions with isotonic internal TEA, the charge was fully recovered in the OFF response. This difference on the action of internal TEA on charge immobilization can arise either from differences in the TEA-binding site located in the internal mouth of the pore (10, 24–26) or in the coupling

mechanisms between the pore and the gating machinery of the channels.

DRK1 ON gating currents showed a slow rising phase that became more prominent with hyperpolarizing prepulses. The existence of a rising phase contradicts the classical model for activation of the squid axon delayed rectifier proposed by Hodgkin and Huxley (27) and extended by Zagotta and Aldrich (28) for Shaker A K<sup>+</sup> channels. In a tetrameric channel model (19), where four identical and independent subunits with two states undergo voltage-dependent structural changes to prepare the channel for opening, gating currents should rise instantaneously and then decay after a single exponential. The slow rising phase in DRK1 ON gating currents discards the hypothesis that identical gating subunits respond to voltage independently and can be explained by independent and nonidentical subunits or by interaction among identical subunits. In this later case, our results are consistent with a model for K<sup>+</sup>-channel activation in which an early slower and/or less voltage-dependent transition between very deep closed states was followed by more voltage-dependent transitions between later closed states. The presence of a deep slower transition was experimentally confirmed with prepulses to less negative potentials (−60 mV), where an instantaneous component was evident, probably due to more voltage-dependent transitions between superficial closed states.

From ionic-current measurements in Shaker A channels, Zagotta and Aldrich (28) proposed that the final closed–open transition is voltage-independent. In agreement with this model, a slow rising phase in Shaker B OFF gating response was recorded for amplitude and pulse durations that opened the channel (6, 13). A similar voltage-independent step may be also present in DRK1 because single-channel measurements showed that the mean open time was practically voltage-independent between −20 and +100 mV. Once the channel has been opened by depolarization, the presence of this final voltage-independent step should delay the return of the gating charge to the nearest closed state. However, this result is not supported by gating measurements because pulses to 0 mV, which clearly should have opened the channel, caused an instantaneous return of the OFF charge and larger depolarizations were necessary to detect the OFF rising phase. This result may indicate that more than one open state in DRK1 channels exists and that only the more distal open transitions are less voltage dependent.

We are indebted to Drs. A. M. Brown and to A. M. J. VanDongen for helpful discussion and to Dr. L. Toro for developing high-

expression DRK1 cRNA. This work was supported by National Institutes of Health Grants (HD25616, NS23877, and HL37044).

- Hille, B. (1992) *Ionic Channels of Excitable Membranes* (Sinauer, Sunderland, MA), 2nd Ed.
- Armstrong, C. M. & Bezanilla, F. (1973) *Nature (London)* **242**, 459–461.
- Bezanilla, F. & Armstrong, C. M. (1975) *Philos. Trans. Roy. Soc. London B* **270**, 449–458.
- White, M. M. & Bezanilla, F. (1985) *J. Gen. Physiol.* **85**, 539–554.
- Spires, S. & Begegnisich, T. (1989) *J. Gen. Physiol.* **93**, 263–283.
- Bezanilla, F., Perozo, E., Papazian, D. M. & Stefani, E. (1991) *Science* **254**, 679–683.
- Frech, G. C., VanDongen, A. M. J., Schuster, G., Brown, A. M. & Joho, R. H. (1989) *Nature (London)* **340**, 642–645.
- Tagliatela, M., Toro, L. & Stefani, E. (1992) *Biophys. J.* **61**, 78–82.
- Tagliatela, M., VanDongen, A. M. J., Drewe, J. A., Joho, R. H., Brown, A. M. & Kirsch, G. E. (1991) *Mol. Pharmacol.* **40**, 299–307.
- Armstrong, C. M. (1966) *J. Gen. Physiol.* **50**, 491–511.
- Kirsch, G. E., Tagliatela, M. & Brown, A. M. (1991) *Am. J. Physiol.* **261**, C583–C590.
- Almers, W. & Armstrong, C. M. (1980) *J. Gen. Physiol.* **75**, 61–78.
- Perozo, E., Papazian, D. M., Stefani, E. & Bezanilla, F. (1992) *Biophys. J.* **62**, 160–171.
- VanDongen, A. M. J., Frech, G. C., Drewe, J. A., Joho, R. A. & Brown, A. M. (1990) *Neuron* **5**, 433–443.
- Hodgkin, A. L. & Katz, B. (1949) *J. Physiol.* **108**, 37–77.
- Almers, W. (1978) *Rev. Physiol. Biochem. Pharmacol.* **82**, 97–190.
- Cole, K. S. & Moore, J. W. (1960) *Biophys. J.* **1**, 161–202.
- Schoppa, N. E., McCormack, K., Tanouye, M. A. & Sigworth, F. J. (1992) *Science* **255**, 1712–1715.
- MacKinnon, R. (1991) *Nature (London)* **350**, 232–235.
- Tytgat, J. & Hess, P. (1992) *Nature (London)* **359**, 420–423.
- Armstrong, C. M. & Bezanilla, F. (1977) *J. Gen. Physiol.* **70**, 567–590.
- Meves, H. & Vogel, W. (1977) *J. Physiol. (London)* **267**, 395–410.
- Stuhmer, W., Conti, F., Stocker, M., Pongs, O. & Heinemann, S. H. (1991) *Pflügers Arch.* **418**, 423–429.
- Yellen, G., Jurman, M. E., Abramson, T. & MacKinnon, R. (1991) *Science* **251**, 939–942.
- Hartmann, H. A., Drewe, J. A., Kirsch, G. E., Tagliatela, M., Joho, R. H. & Brown, A. M. (1991) *Science* **251**, 942–944.
- Kirsch, G. E., Drewe, J. A., Hartman, H., Tagliatela, M., DeBiasi, M. & Brown, A. M. (1992) *Neuron* **8**, 499–505.
- Hodgkin, A. L. & Huxley, A. F. (1952) *J. Physiol. (London)* **117**, 500–544.
- Zagotta, W. N. & Aldrich, R. W. (1990) *J. Gen. Physiol.* **95**, 29–60.